2018 Australian & New Zealand Control Conference (ANZCC)
Swinburne University of Technology
Melbourne, Australia, Dec 7-8, 2018

AUV navigation with seabed acoustic sensing*

Alexander Miller[1], Boris Miller[1] and Gregory Miller[2]

KEYWORDS

AUV; acoustic sensing; navigation.

ABSTRACT

Autonomous Underwater Vehicle (AUV) being a powerful tool for exploring and investigating ocean resources can be used in a large variety of oceanographic, industry and defense applications. AUV navigation is still a challenging task and it is one of the fundamental elements in the modern robotics, because the ability of AUV to correctly understand its position and attitude within the underwater environment is determinant for success in different applications. Due to the absence of external reference sources, AUV navigation is usually based only on the information obtained from Doppler Velocity Loggers (DVL), Inertial Navigation Systems (INS), etc. But this type of navigation is subjected to a continuously growing error because of the absence of absolute position measurements (for example, received from the GPS or GLONASS). These measurements might be provided by observation of so-called feature points like in the case of the Unmanned Aerial Vehicles (UAV). But the big difference between acoustical and optical images makes this problem much more difficult in the AUV case, and to solve it one needs the detailed preliminary mapping of the operational seabed area. The modern advances in the acoustic imaging give rise to AUV navigation approaches based on the absolute velocity measurements. The one we propose in the present paper is analogous to the optical flow techniques for UAV navigation. It is based on the extraction of information related to the AUV absolute motion from seabed map evolution measurements. The principal advantage of the proposed method is that the fusion of the acoustic mapping and the INS data makes it possible to estimate the absolute velocity of the vehicle with respect to the seabed. In this sense the suggested method is close to the multi-beam DVL measurement, but it is based on another physical principles and thus operates better in different environment. While DVL by design operates perfectly over the flat surface [1], the appropriate environment for the suggested method implicates the seabed relief, because it extracts the velocity information from the evolution of the measured distance between the sensor and the seabed.

I. INTRODUCTION

Nowadays sonars are used in various application fields from tracking of mobile objects to inspecting underwater communication lines [2]. Sonars are very useful for obstacle collisions avoiding as well as for detection of characteristic objects located on the seabed [2], [3], [4]. Modern sonars make it possible to obtain acoustic images of the seabed and the surrounding space, and this data can be used for solving navigational problems [5]. Application of sonars for AUV selflocalization is possible by analogy with UAV: the necessary data may be extracted from the comparison of the recorded bottom relief with the preloaded seabed map [6]. Optical flow navigation techniques for UAV are based on linking of the vehicle movement and the speed of the image shift in the focal plane [7], [8], [9]. Application of the same concepts for AUV navigation implies the derivation of the relations that allow to extract the speed of the AUV motion from the sequence of the seabed distance measurements obtained from sonars. This derivation is not straightforward and various problems arise with acoustic images processing [10]. One of the problems is that the calculation of the AUV shift using the evolution of the measured seabed profile from frame to frame is only possible when the relief characteristics, i.e. slopes, are known, but if AUV operates over the unknown seabed (which is a most usual case), these parameters are subject to determination.

There are various approaches to the AUV navigation basing on acoustic imaging [11], [12], [13]. The relations between the vehicle motion and the acoustic images evolution may be derived in the form that connects the measured relief distance change rate with the AUV velocities. The ability to perform measurements over a wide range of angles yields a system of equations, where three velocity components are related to the seabed distances measured at different angles. If the number of observations is much bigger than the number of estimated elements of motion, the latter may be estimated fairly accurately by means of the least squares method, which thus becomes the basis of proposed algorithm.

In this article we demonstrate a new approach to the AUV absolute velocity estimation based on the observation of the evolution of the series of acoustical images captured by sonar at relatively wide observation angle. In the section II the mathematical model of the AUV motion and acoustic sensor observations is presented. Section III contains the solution to the AUV velocity estimation problem. In order to demonstrate the quality of the proposed algorithm, in section IV

*This work was partially supported by Russian Foundation for Basic Research (grants 16-31-60049, 16-08-01076, and 16-07-00677).

[1]Alexander Miller and Boris Miller are with Institute for Information Transmission Problems RAS, Moscow, Russia {amiller, bmiller}@iitp.ru

[2]Gregory Miller is with Federal Research Center "Computer Science and Control" RAS, Moscow, Russia gmiller@frccsc.ru

**Boris Miller is Adjunct Senior Research Fellow of Monash University, VIC, Australia

an illustrative modeling example of AUV perturbed motion parameters estimation given the set of seabed distance noisy measurements is provided.

II. AUV MOTION MODEL

In this section we present a model of AUV motion in 3D space under the water surface and the seabed acoustic image sequence acquisition and processing. We assume that at time t_j AUV echo locator produces a set of measurements of the distance from the vehicle to the seabed $L(\mathbf{X}(t_j), \bar{\mathbf{e}}(\phi_i, \theta_k))$ were

- vector $\mathbf{X}(t_j)$ stands for the AUV coordinates in 3D space
$$\mathbf{X}(t_j) = \begin{pmatrix} X(t_j) \\ Y(t_j) \\ Z(t_j) \end{pmatrix},$$
- vector $\bar{\mathbf{e}}(\phi_i, \theta_k)$ defines the direction of a single (i,k)-th acoustic beam in Cartesian coordinate system:
$$\bar{\mathbf{e}}(\phi_i, \theta_k) = \begin{pmatrix} e_x(\phi_i, \theta_k) \\ e_y(\phi_i, \theta_k) \\ e_z(\phi_i, \theta_k) \end{pmatrix} = \begin{pmatrix} \sin\phi_i \cos\theta_k \\ \sin\phi_i \sin\theta_k \\ -\cos\phi_i \end{pmatrix},$$
- angles (ϕ_i, θ_k) define the direction of the (i,k)-th beam in spherical coordinate system with origin at the AUV. It is supposed that AUV uses set of $N \cdot N$ acoustic beams, $i, k = 1, \ldots, N$ (See Fig. 1).

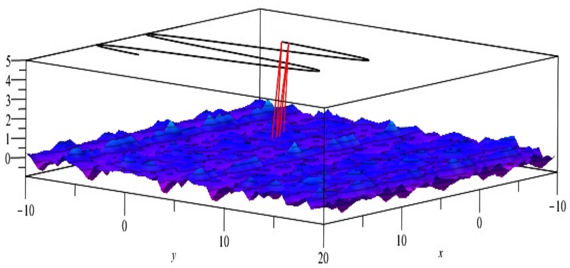

Fig. 1. 3D model of AUV motion. Black is the trajectory of the AUV over the seabed. The acoustic beams are depicted with red lines.

At time t_j AUV position is $\mathbf{X}(t_j)$ so the measurement signal in direction $\bar{\mathbf{e}}(\phi_i, \theta_k)$ reaches the bottom at the point (x, y, z) (See Fig. 2):

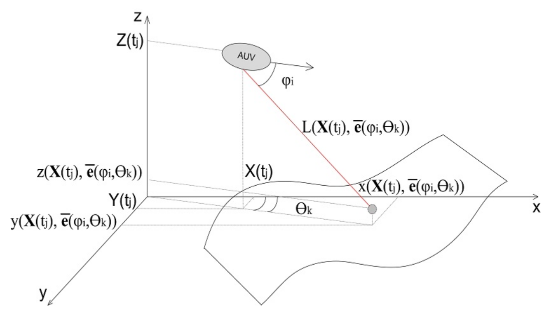

Fig. 2. AUV at the moment t_j reaching the bottom point (x, y, z) with the acoustic beam $L(\mathbf{X}(t_j), \bar{\mathbf{e}}(\phi_i, \theta_k))$.

$$\begin{pmatrix} x(\mathbf{X}(t_j), \bar{\mathbf{e}}(\phi_i, \theta_k)) \\ y(\mathbf{X}(t_j), \bar{\mathbf{e}}(\phi_i, \theta_k)) \\ z(\mathbf{X}(t_j), \bar{\mathbf{e}}(\phi_i, \theta_k)) \end{pmatrix} = \begin{pmatrix} X(t_j) \\ Y(t_j) \\ Z(t_j) \end{pmatrix}$$
$$+L(\mathbf{X}(t_j), \bar{\mathbf{e}}(\phi_i, \theta_k)) \begin{pmatrix} e_x(\phi_i, \theta_k) \\ e_y(\phi_i, \theta_k) \\ e_z(\phi_i, \theta_k) \end{pmatrix}.$$

Assuming the seabed profile is unknown and given by some smooth function $z = z(x, y)$ we can write:

$$Z(t_j) + e_z(\phi_i, \theta_k) L(\mathbf{X}(t_j), \bar{\mathbf{e}}(\phi_i, \theta_k))$$
$$= z\Big(X(t_j) + e_x(\phi_i, \theta_k) L(\mathbf{X}(t_j), \bar{\mathbf{e}}(\phi_i, \theta_k)), \qquad (1)$$
$$Y(t_j) + e_y(\phi_i, \theta_k) L(\mathbf{X}(t_j), \bar{\mathbf{e}}(\phi_i, \theta_k))\Big).$$

Differentiating this equation by t we get:

$$\frac{dZ}{dt} + e_z \frac{dL}{dt} = \frac{\partial z}{\partial x}\left(\frac{dX}{dt} + e_x \frac{dL}{dt}\right) + \frac{\partial z}{\partial y}\left(\frac{dY}{dt} + e_y \frac{dL}{dt}\right). \qquad (2)$$

In this equation the derivatives $\frac{dX}{dt}$, $\frac{dY}{dt}$ and $\frac{dZ}{dt}$ define AUV velocities along the axis x, y and z respectively. In the next section we provide algorithm of these elements evaluation.

III. AUV MOTION ESTIMATION

The algorithm of the AUV velocities evaluation in fact gives the estimates of the AUV shift between the time instants t_j and t_{j-1}. The algorithm consists of the following steps, which are performed at each time instant t_j:

1) evaluate $\frac{dL}{dt}$ using successive distance measurements from the equally aimed echo locator beams $L(\mathbf{X}(t_{j-1}), \bar{\mathbf{e}}(\phi_i, \theta_k))$ and $L(\mathbf{X}(t_j), \bar{\mathbf{e}}(\phi_i, \theta_k))$;
2) for each beam direction (ϕ_i, θ_k), $i, k = 1, \ldots, N$ evaluate the partial derivatives of the seabed profile function $\frac{\partial z}{\partial x}(\phi_i, \theta_k)$, $\frac{\partial z}{\partial y}(\phi_i, \theta_k)$ (i.e. slopes). With slight abuse of notation the dependence on the beam direction is further omitted, and the slopes are estimated in accordance with the following considerations:
   - taking the partial derivatives $\frac{\partial}{\partial e_x}$, $\frac{\partial}{\partial e_y}$ and $\frac{\partial}{\partial e_z}$ in the equation (1) yields the following system:
$$\frac{\partial z}{\partial x}\left(L + e_x \frac{\partial L}{\partial e_x}\right) + \frac{\partial z}{\partial y}\left(L \frac{\partial e_y}{\partial e_x} + e_y \frac{\partial L}{\partial e_x}\right)$$
$$= \frac{\partial e_z}{\partial e_x} L + e_z \frac{\partial L}{\partial e_x},$$
$$\frac{\partial z}{\partial x}\left(L \frac{\partial e_x}{\partial e_y} + e_x \frac{\partial L}{\partial e_y}\right) + \frac{\partial z}{\partial y}\left(L + e_y \frac{\partial L}{\partial e_y}\right)$$
$$= \frac{\partial e_z}{\partial e_y} L + e_z \frac{\partial L}{\partial e_y},$$

$$\frac{\partial z}{\partial x}\left(e_x\frac{\partial L}{\partial e_z}+\frac{\partial e_x}{\partial e_z}L\right)+\frac{\partial z}{\partial y}\left(e_y\frac{\partial L}{\partial e_z}+\frac{\partial e_y}{\partial e_z}L\right)$$
$$=e_z\frac{\partial L}{\partial e_z}+L,$$

- this system may be rewritten in a simpler form by introducing new notation:
$$\begin{pmatrix} a & b \\ f & g \\ q & w \end{pmatrix}\begin{pmatrix} \frac{\partial z}{\partial x} \\ \frac{\partial z}{\partial y} \end{pmatrix}=\begin{pmatrix} c \\ h \\ p \end{pmatrix},$$
where
$$a=L(\mathbf{X}(t_j),\bar{\mathbf{e}}(\phi_i,\theta_k))+e_x(\phi_i,\theta_k)\frac{\partial L}{\partial e_x},$$
$$b=-L(\mathbf{X}(t_j),\bar{\mathbf{e}}(\phi_i,\theta_k))\frac{\cos\theta_k}{\sin\theta_k}+e_y(\phi_i,\theta_k)\frac{\partial L}{\partial e_x},$$
$$c=L(\mathbf{X}(t_j),\bar{\mathbf{e}}(\phi_i,\theta_k))\frac{\sin\phi_i\cos\theta_k}{\cos\phi_i}+e_z(\phi_i,\theta_k)\frac{\partial L}{\partial e_x},$$
$$f=-L(\mathbf{X}(t_j),\bar{\mathbf{e}}(\phi_i,\theta_k))\frac{\sin\theta_k}{\cos\theta_k}+e_x(\phi_i,\theta_k)\frac{\partial L}{\partial e_y},$$
$$g=L(\mathbf{X}(t_j),\bar{\mathbf{e}}(\phi_i,\theta_k))+e_y(\phi_i,\theta_k)\frac{\partial L}{\partial e_y},$$
$$h=L(\mathbf{X}(t_j),\bar{\mathbf{e}}(\phi_i,\theta_k))\frac{\sin\phi_i\sin\theta_k}{\cos\phi_i}+e_z(\phi_i,\theta_k)\frac{\partial L}{\partial e_y},$$
$$q=e_x(\phi_i,\theta_k)\frac{\partial L}{\partial e_z}+L(\mathbf{X}(t_j),\bar{\mathbf{e}}(\phi_i,\theta_k))\frac{\cos\phi_i}{\sin\phi_i\cos\theta_k},$$
$$w=e_y(\phi_i,\theta_k)\frac{\partial L}{\partial e_z}+L(\mathbf{X}(t_j),\bar{\mathbf{e}}(\phi_i,\theta_k))\frac{\cos\phi_i}{\sin\phi_i\sin\theta_k},$$
$$p=e_z(\phi_i,\theta_k)\frac{\partial L}{\partial e_z}+L(\mathbf{X}(t_j),\bar{\mathbf{e}}(\phi_i,\theta_k)),$$
and
$$\frac{\partial L}{\partial e_x}=\frac{L(\mathbf{X}(t_j),\bar{\mathbf{e}}(\phi_i,\theta_k))-L(\mathbf{X}(t_j),\bar{\mathbf{e}}(\phi_{i-1},\theta_k))}{e_x(\phi_i,\theta_k)-e_x(\phi_{i-1},\theta_k)},$$
$$\frac{\partial L}{\partial e_y}=\frac{L(\mathbf{X}(t_j),\bar{\mathbf{e}}(\phi_i,\theta_k))-L(\mathbf{X}(t_j),\bar{\mathbf{e}}(\phi_i,\theta_{k-1}))}{e_x(\phi_i,\theta_k)-e_x(\phi_i,\theta_{k-1})},$$
$$\frac{\partial L}{\partial e_z}=(L(\mathbf{X}(t_j),\bar{\mathbf{e}}(\phi_{i-1},\theta_k))-L(\mathbf{X}(t_j),\bar{\mathbf{e}}(\phi_{i-1},\theta_{k-1}))$$
$$+L(\mathbf{X}(t_j),\bar{\mathbf{e}}(\phi_i,\theta_{k-1}))-L(\mathbf{X}(t_j),\bar{\mathbf{e}}(\phi_i,\theta_k)))$$
$$\times\frac{e_z(\phi_i,\theta_k)}{e_x(\phi_i,\theta_k)\Delta e_x+e_y(\phi_i,\theta_k)\Delta e_y},$$
$$\Delta e_x=e_x(\phi_i,\theta_k)-e_x(\phi_{i-1},\theta_k),$$
$$\Delta e_y=e_y(\phi_i,\theta_k)-e_y(\phi_i,\theta_{k-1}),$$

- further with notation
$$A=\begin{pmatrix} a & b \\ f & g \\ q & w \end{pmatrix},\quad B=\begin{pmatrix} c \\ h \\ p \end{pmatrix},$$
the original system is represented in the following matrix form
$$A\begin{pmatrix} \frac{\partial z}{\partial x} \\ \frac{\partial z}{\partial y} \end{pmatrix}=B,$$
- finally the solution of the above system yields the relations for the partial derivatives $\frac{\partial z}{\partial x}$, $\frac{\partial z}{\partial y}$:
$$\begin{pmatrix} \frac{\partial z}{\partial x} \\ \frac{\partial z}{\partial y} \end{pmatrix}=[A^TA]^{-1}[A^TB],$$
where
$$[A^TA]^{-1}=\frac{1}{\det[A^TA]}$$
$$\times\begin{pmatrix} b^2+g^2+w^2 & -(ab+fg+qw) \\ -(ab+fg+qw) & a^2+f^2+q^2 \end{pmatrix},$$
$$\det[A^TA]$$
$$=(a^2+f^2+q^2)(b^2+g^2+w^2)$$
$$-(ab+fg+qw)^2,$$
$$A^TB=\begin{pmatrix} ac+fh+qp \\ bc+gh+wp \end{pmatrix};$$

3) finally estimate $\frac{dX}{dt}$, $\frac{dY}{dt}$, $\frac{dZ}{dt}$ knowing the set of slope estimations $\frac{\partial z}{\partial x}$ and $\frac{\partial z}{\partial y}$ for every beam direction (ϕ_i,θ_k), $i,k=1,\ldots,N$:

- rewriting (2) with representing the derivatives via increments yields the equation
$$\Delta Z(t_j)-\frac{\partial z}{\partial x}\Delta X(t_j)-\frac{\partial z}{\partial y}\Delta Y(t_j)$$
$$=-\Delta L(\mathbf{X}(t_j),\bar{\mathbf{e}}(\phi_i,\theta_k))$$
$$\times\left(e_z(\phi_i,\theta_k)-\frac{\partial z}{\partial x}e_x(\phi_i,\theta_k)-\frac{\partial z}{\partial y}e_y(\phi_i,\theta_k)\right),$$
and further with the following notation
$$M=-e_z(\phi_i,\theta_k)+\frac{\partial z}{\partial x}e_x(\phi_i,\theta_k)+\frac{\partial z}{\partial y}e_y(\phi_i,\theta_k)$$
it may be rewritten in the form
$$\Delta Z(t_j)-\frac{\partial z}{\partial x}\Delta X(t_j)-\frac{\partial z}{\partial y}\Delta Y(t_j)$$
$$=M\Delta L(\mathbf{X}(t_j),\bar{\mathbf{e}}(\phi_i,\theta_k)),$$

- finally the shifts $\Delta X(t_j), \Delta Y(t_j), \Delta Z(t_j)$ can be estimated with the aid of least square method:

$$\sum_{i=1}^{N}\sum_{k=1}^{N}\Big(\Delta\hat{Z}(t_j) - \frac{\partial z}{\partial x}\Delta\hat{X}(t_j) - \frac{\partial z}{\partial y}\Delta\hat{Y}(t_j) - M\Delta L(\mathbf{X}(t_j), \bar{\mathbf{e}}(\phi_i,\theta_k))\Big)^2 \to \min_{\Delta\hat{X}(t_j),\Delta\hat{Y}(t_j),\Delta\hat{Z}(t_j)}$$

Standard calculations give the following equation for the estimates of the AUV shift between the time instants t_j and t_{j-1}:

$$\Delta\hat{\mathbf{X}}(t_j) = \begin{pmatrix} \Delta\hat{X}(t_j) \\ \Delta\hat{Y}(t_j) \\ \Delta\hat{Z}(t_j) \end{pmatrix} = [\tilde{\mathbf{B}}]^{-1}\tilde{\mathbf{M}},$$

where

$$\tilde{\mathbf{B}} = \begin{pmatrix} \sum\left(\frac{\partial z}{\partial x}\right)^2 & \sum\frac{\partial z}{\partial x}\frac{\partial z}{\partial y} & -\sum\frac{\partial z}{\partial x} \\ \sum\frac{\partial z}{\partial x}\frac{\partial z}{\partial y} & \sum\left(\frac{\partial z}{\partial y}\right)^2 & -\sum\frac{\partial z}{\partial y} \\ -\sum\frac{\partial z}{\partial x} & -\sum\frac{\partial z}{\partial y} & \sum 1 \end{pmatrix},$$

$$\tilde{\mathbf{M}} = \begin{pmatrix} \sum M\Delta L(\mathbf{X}(t_j), \bar{\mathbf{e}}(\phi_i,\theta_k))\frac{\partial z}{\partial x} \\ \sum M\Delta L(\mathbf{X}(t_j), \bar{\mathbf{e}}(\phi_i,\theta_k))\frac{\partial z}{\partial y} \\ -\sum M\Delta L(\mathbf{X}(t_j), \bar{\mathbf{e}}(\phi_i,\theta_k)) \end{pmatrix},$$

and symbol $\sum$ stands for $\sum\limits_{i=1}^{N}\sum\limits_{k=1}^{N}$.

IV. Modelling

In order to evaluate the quality of the AUV velocities estimation algorithms a series of numerical simulations was performed.

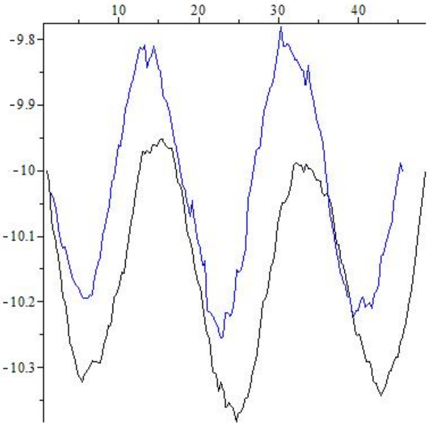

Fig. 3. Tracking of the 2D AUV motion

First we consider a two dimensional case with the AUV moving in the vertical plane. The modelling setting is thus as follows.

- AUV is moving from point $(X_0, Z_0) = (1, -10)$ to the (X_T, Z_T);
- motion along X axis is with constant velocity $0.3\frac{m}{s}$ and the motion along axis Z is with harmonically changing velocity with the amplitude $0.02\frac{m}{s}$;
- motion is perturbed by white noise with intensities $\sigma(a_x) = 0.06\frac{m}{s^2}$ and $\sigma(a_z) = 0.02\frac{m}{s^2}$ for horizontal and vertical components respectively;
- accuracy of the range measurement assumed $0.1m$, which corresponds to the sonar's accuracy for the depth of the order $10m$;
- number of measurements made in each point of trajectory (the number of beams) is $N = 80$;
- direction of the i-th measurement beam is $\phi_i = 0.0285(i+1)\frac{\pi}{10}$;
- unknown seabed profile is given by the following smooth function $z(x) = -20 + 0.001x^2 - 0.3\sin(2.5x)$.

Fig. 3 shows a sample of AUV trajectory (black) and its estimate (blue). Table I contains the results of Monte-Carlo modelling with $k = 100$ sample trajectories. For time instants $t_j = 20, 40, 80, 160$ seconds mean $(E_X(t_j), E_Z(t_j))$ and standard deviation $(\sigma_X(t_j), \sigma_Z(t_j))$ of the estimation errors are provided.

Fig. 4 shows the AUV moving under the seabed and performing range measurements in the beginning of its mission and in the end. The black is the real AUV trajectory and the red is the estimate. Bold are the points where the acoustic beams meet the seabed.

TABLE I
Statistics of estimation errors

t_j	$E_X(t_j)$	$E_Z(t_j)$	$\sigma_X(t_j)$	$\sigma_Z(t_j)$
20	-0.1636	0.0554	0.2157	0.0740
40	-0.6625	0.0810	0.6861	0.1058
80	0.0810	0.1427	1.5632	0.1851
160	-3.3115	-0.1446	3.3371	0.2721

In the next example the AUV is moving in 3D space and the modelling setting differs from the previous one in the following points:

- AUV is moving from point $(X_0, Y_0, Z_0) = (1, 0, -10)$ to the (X_T, Y_T, Z_T);
- motion along X and Z axis is the same, while along the Y axis the AUV moves with constant velocity $0.3\frac{m}{s}$;
- motion along the Y axis is perturbed by white noise with intensity $\sigma(a_y) = 0.03\frac{m}{s^2}$, the motion perturbations along X and Z axes are the same;
- sonar accuracy is the same $(0.1m)$;
- number of measurements made in each point of trajectory is equal to $N = 100$, which means that the AUV uses a set of $10 \cdot 10$ acoustic beams;

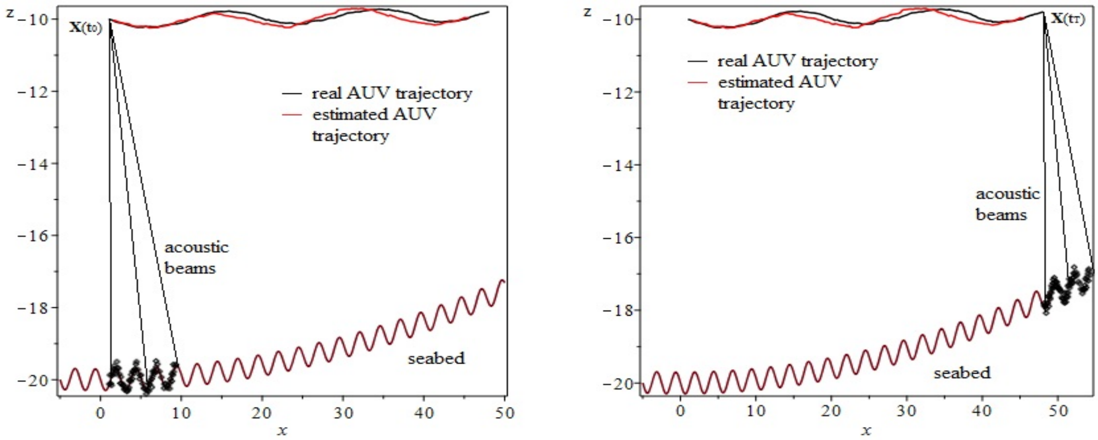

Fig. 4. AUV moving under the seabed and performing range measurements, on the left — at the time instant t_0, on the right — at time instant t_T. Bold are the points of the seabed used for acoustic sensing.

- direction of the i-th measurement beam is $\phi_i = \frac{2\pi}{45} + (i+1)\frac{\pi}{45}$;
- direction of the k-th measurement beam varies for different components: $\theta_k = \frac{2\pi}{9} + (k+1)\frac{\pi}{90}$ for estimation of the shift along the axis X, $\theta_k = \frac{13\pi}{9} + (k+1)\frac{\pi}{90}$ for shift along the axis Y, and $\theta_k = \frac{17\pi}{18} + (k+1)\frac{\pi}{90}$ for axis Z. In fact this setting corresponds to three sensor groups aiming in different directions. As it would be clear from the results, such a diversity positively affects the estimation quality.
- unknown seabed profile is given by the following smooth function $z(x) = -20 + 0.001x^2 - 0.3\sin(2.5x) - 0.002y^2 + 0.2\cos(1.5y)$.

Fig. 5 shows a sample of 3D AUV trajectory (black) and its estimate (blue). Table II contains the results of Monte-Carlo modelling with $k = 100$ sample trajectories. For the same time instants as in 2D case, the mean $(E_X(t_j), E_Y(t_j), E_Z(t_j))$ and standard deviation $(\sigma_X(t_j), \sigma_Y(t_j), \sigma_Z(t_j))$ of the estimation errors are provided. The comparison of the obtained results shows better performance of the algorithm for 3D case with $10 \cdot 10$ beams distributed over a surface than for 2D case with only slightly less number of beams (80) aligned along a single plane. It should be noted that this is a consequence of using separate sensors aimed in different direction for estimation of the shifts along axes X, Y, Z. Using the same direction for estimation of all three components yields significantly worse results. Thus clever positioning and aiming of the acoustic sensors is a significant issue and it will definitely be addressed in the future research.

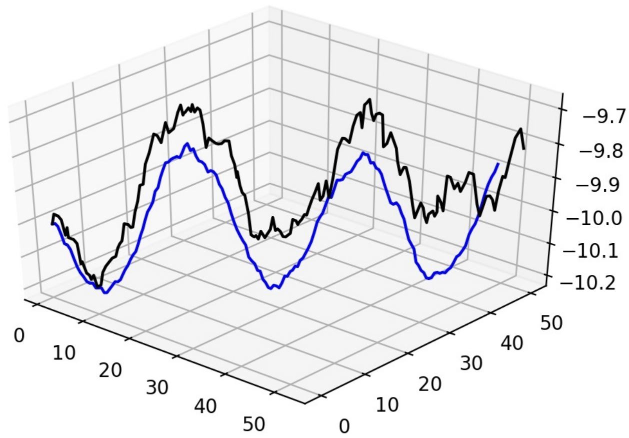

Fig. 5. Tracking of the 3D AUV motion

TABLE II
STATISTICS OF ESTIMATION ERRORS

t_j	$E_X(t)$	$E_Y(t)$	$E_Z(t)$	$\sigma_X(t)$	$\sigma_Y(t)$	$\sigma_Z(t)$
20	-0.9720	0.8572	0.0133	0.1859	0.4642	0.0286
40	-0.9878	2.5233	0.0715	0.2684	0.6549	0.0420
80	-1.6778	3.0574	0.1196	0.4305	0.9120	0.0566
160	2.8369	3.6124	0.1473	0.5364	1.0840	0.1593

V. Conclusion

In this work we obtained the relations that allow to extract the AUV velocities from the sequence of acoustic images. These relations are presented in a form connecting the rate of change of the measured distance between AUV and the seabed with the components of the AUV velocity. This particular representation allowed to design an algorithm for AUV velocity components estimation. The core feature of this algorithm is the least squares approximation performed over the set of seabed distance observations collected at different directions. The proposed algorithm was examined in 2D case with AUV movement allowed only in vertical plane and in a full 3D setting. Both modelling examples showed good estimation quality, but gave rise to another problem of beam aiming optimization. This problem, along with other means of increasing the AUV position estimation quality, such as integration with INS, we plan to address in our future research. It should be emphasized that navigation based on velocities measurements only inevitably leads to the drift in position estimation. The latter may be compensated, for example, by referencing to some objects or parts of the seabed with known positions. This techniques had already been tested in UAV navigation [7] and seem quite promising for underwater applications.

REFERENCES

[1] *Dylan Rudolph and Timothy A. Wilson* Doppler Velocity Log Theory and Preliminary Considerations for Design and Construction. Proceedings of IEEE Southeastcon 15-18 March 2012, ieeexplore.ieee.org/document/6196918/, DOI: 10.1109/SECon.2012.6196918.

[2] *Filip Mandic, Ivor Renduligravec, Nikola Miskovigravec, and Dula Nad* Underwater Object Tracking Using Sonar and USBL Measurements. Hindawi Publishing Corporation Journal of Sensors Vol. 2016, Article ID 8070286, pp. 1–10 http://dx.doi.org/10.1155/2016/8070286

[3] *K.B. Anonsen and O. Hallingstad* Terrain Aided Underwater Navigation Using Point Mass and Particle Filters. Procedings of 2006 IEEE/ION Position, Location, And Navigation Symposium 2006, pp.1027–1035.

[4] Pengyun Chen, Ye Li, Yumin Su, Xiaolong Chen and Yanqing Jiang, *Review of AUV Underwater Terrain Matching Navigation*, The Journal of Navigation 2015, Vol. 68, pp. 1155–1172.

[5] *Puneet Singh, Anuj Sehgal, Parth Shah and Jason Kadarusman* Autonomous Underwater Unmanned Vehicular Recovery System based on Low-Cost Inter-Aural Time Differentiation Passive Sonar. Proceedings of 2007, Mediteranian Conference on Control and Automation, Athens, Greece July 27-29, T34-003.

[6] *Ziqi Song, Hongyu Bian, and Adam Zielinski* Application of acoustic image processing in underwater terrain aided navigation. Ocean Engineering, Vol. 121(2016) pp. 279-290

[7] S. Karpenko, I. Konovalenko, A. Miller, B. Miller and D. Nikolaev, *UAV Control on the Basis of 3D Landmarks Bearing-Only Observations*, Sensors. 2015. Vol. 15. No. 12. pp. 29802–29820. http://dx.doi.org/10.3390/s151229768.

[8] *A. Popov, B. Miller, A. Miller, and K. Stepanyan* Optical Flow as a Navigation Means for UAVs with Opto-electronic Cameras // Proceedings of 56th Israel Annual Conference on Aerospace Sciences, March 9-10, Tel-Aviv and Haifa, Israel. 2016. ThL2T5.2.

[9] *A. Popov, A. Miller, B. Miller, and K. Stepanyan* Optical Flow and Inertial Navigation System Fusion in UAV Navigation // International Conference Defence and Security, Unmanned/Unattended Sensors and Sensor Networks XII, September 26, Edinburgh, United Kingdom. 2016. Proceedings of SPIE. V. 9986. P. 998606-(1–16). http://dx.doi.org/10.1117/12.2241204

[10] *Andrea Caiti, Francesco Di Corato, Davide Fenucci, Benedetto Allotta, Fabio Bartolini, Riccardo Costanzi, Jonathan Gelli, Niccolo Monni, Marco Natalini, Luca Pugi, and , Alessandro Ridolfi* Fusing acoustic ranges and inertial measurements in AUV navigation: The Typhoon AUV at CommsNet13 sea trial. OCEANS 2014 - TAIPEI, April 2014, pp.1-5

[11] *S. A. Villar, G. G. Acosta, A. L. Sousa, and A. Rozenfeld* Evaluation of an Efficient Approach for Target Tracking from Acoustic Imagery for the Perception System of an Autonomous Underwater Vehicle. International Journal of Advanced Robotic Systems, vol. 11, (2), 2014.

[12] *Hua Lee* Optimization of computation efficiency in underwater acoustic navigation system. The Journal of the Acoustical Society of America 2016, Vol. 139, pp. 1909–1913. DOI: 10.1121/1.4945099

[13] *S. E Webster, R. M. Eustice, H. Singh, L. L. Whitcomb* Advances in single-beacon one-way-travel-time acoustic navigation for underwater vehicles. The International Journal of Robotics Research 2012. Vol. 31(8) pp. 935–949. DOI: 10.1177/0278364912446166